Impulse response of a nonlinear dispersive wave

M. Yu and C. J. McKinstrie
Department of Mechanical Engineering, University of Rochester, Rochester, New York 14627
and Laboratory for Laser Energetics, 250 East River Road, Rochester, New York 14623
(Received 2 June 1995)

The spatiotemporal instability of a nonlinear wave is studied by applying impulse-response analysis. The time-asymptotic Green function is obtained analytically for both modulationally stable and unstable cases. The conditions for absolute and convective instability are found analytically, as is the frequency region for amplification and the spatial and temporal growth rates.

PACS number(s): 42.81.Dp, 52.35.Mw, 42.65.Ky

I. INTRODUCTION

The nonlinear Schrödinger equation (NSE) is widely used to describe nonlinear dispersive wave propagation occurring in many branches of physics and engineering, such as plasma physics, nonlinear optics, and fluids dynamics. One of the prominent features associated with the NSE is the existence of modulational instability (MI), which causes small modulations of a plane wave propagating in a dispersive Kerr medium to grow exponentially. For a tutorial introduction to modulational instabilities and a short bibliography of original papers, see Ref. [1]. Longer bibliographies can be found in Refs. [2–4].

A fundamental characterization for any unstable (or stable) dispersive system is the asymptotic spatiotemporal behavior of a small localized perturbation. Such an asymptotic impulse-response study can provide much important information, including the classification of the instability as convective or absolute and the differentiation between evanescent and amplified waves. In fact, the asymptotic impulse-response study has been performed on most common instabilities in both plasmas and fluids, and the results can be found in standard textbooks [5–8]. However, for the important case of a nonlinear dispersive wave, this aspect of study was only partially done [1,9]. This paper aims to fill the gap in the literature by analytically studying the impulse response of a nonlinear plane wave in a dispersive Kerr medium. Some features pertinent to such a system as revealed by our impulse-response study are discussed.

II. IMPULSE RESPONSE

The NSE can be written as [1]

$$\partial_{t'}a=-v_g'\partial_{x'}a-i\mu\partial_{x'x'}^2a+i\lambda|a|^2a\ , \tag{1}$$

where a is the complex field, x' and t' are the spatial and temporal coordinates, v_g' is the group velocity, μ is the dispersion coefficient, and γ is the nonlinear coefficient.

Equation (1) has a plane-wave solution $a_p(x,t)=a_0\exp(i\lambda a_0^2t)$, where a_0 is a complex constant representing the amplitude and phase of the plane wave. Without loss of generality, we assume a_0 to be a real positive quantity since its phase can always be canceled by a time translation. We will also assume λ is positive since the discussion for the negative case is quite similar. If we introduce the normalizations $A=a/a_0$, $x=x'a_0\sqrt{\lambda/|\mu|}$, $t=t'\lambda a_0^2$, and $v_g=v_g'/\sqrt{a_0^2\lambda|\mu|}$, Eq. (1) can be written in the normalized form

$$\partial_tA=-v_g\partial_xA-i\sigma\partial_{xx}^2A+i|A|^2A\ , \tag{2}$$

and the plane-wave solution becomes $A_p=\exp(it)$. We have used $\sigma=\mathrm{sgn}(\mu)$ to simplify the notation.

The evolution of the perturbative field is governed by Eq. (2) linearized around the plane-wave solution. Using $A=(1+\delta A)\exp(it)$ in Eq. (2) and linearizing for δA, we obtain

$$\delta_t\delta A+v_g\partial x\delta A+i\sigma\partial_{xx}^2\delta A-i\delta A-i\delta A^*=0. \tag{3}$$

For the impulse-response analysis of the linearized equation, we need to solve the initial value problem of

$$\partial_t\delta A+v_g\partial_x\delta A+i\sigma\partial_{xx}^2\delta A-i\delta A-i\delta A^*=S(t)\delta(x)\ , \tag{4}$$

with $\delta A(x,t)=0$ for $t<0$, where $S(t)\delta(x)$ is the point source of the perturbation. Equation (4) is readily solved by applying Fourier and Laplace transforms in x and t. The result is

$$i(-\omega+kv_g-\sigma k^2-1)\overline{\delta A}(\omega,k)-i[\overline{\delta A}(-\omega^*,-k)]^*=\bar{S}(\omega)\ . \tag{5}$$

Since the above equation holds for arbitrary ω and k, we take its complex conjugate and replace ω and k with $-\omega^*$ and $-k$, respectively:

$$-i(\omega-kv_g-\sigma k^2-1)[\overline{\delta A}(-\omega^*,-k)]^*+i\overline{\delta A}(\omega,k)=[\bar{S}(-\omega_*)]^*\ . \tag{6}$$

Using Eqs. (5) and (6), we obtain the solution

$$\overline{\delta A}(\omega,k)=i\frac{(\omega-v_gk-\sigma k^2-1)\bar{S}(\omega)-[\bar{S}(-\omega^*)]^*}{(\omega-v_gk)^2-\sigma k^2(1+\sigma k^2)}\ . \tag{7}$$

Its inverse transform is given by

$$\delta A(x,t)=\int \frac{dk}{2\pi}\int_L \frac{d\omega}{2\pi} e^{-i\omega t+ikx}\overline{\delta A}(\omega,k)\,, \tag{8}$$

where the integration paths of k and ω are the real axis and Landau contour (for the inverse Laplace transform, see [6]), respectively.

III. ASYMPTOTIC PULSE EVOLUTION

We first consider $S(t)=c\delta(t)$, where c is generally a complex constant. In such a case, the Green function obtained from Eq. (8) corresponds to the evolution of a δ pulsed perturbation. The evolution of a general pulse can be studied in terms of its convolution. For simplicity, we assume $c=1$ so that $\bar{S}(\omega)=1$. We concern ourselves with the asymptotic spatiotemporal behavior of the Green function. Thus we assume t is very large and work with a spatial coordinate normalized to t, i.e., $v=x/t$. In such a limit, the integrations in Eq. (8) can be carried out approximately. There are two equivalent approaches. Basically, the first one is to conceptually integrate k first and approximate the final integration of ω by the contributions from its branch points in the integrand. The second one is to integrate ω first and approximate the final integration of k by the contributions from its saddle points in the exponentials (i.e., by steepest descent integration). We adopt the second approach here. After carrying out the integration in Eq. (8) with respect to ω by summation of its simple poles at

$$\omega=v_g k\pm k\sqrt{k^2+2\sigma} \tag{9}$$

in Eq. (7), we have

$$\delta A(vt,t)=\int \frac{dk}{2\pi}\exp[ikv't]\left\{[\exp(itk\sqrt{k^2+2\sigma})+\exp(-itk\sqrt{k^2+2\sigma})]/2 + \sigma\frac{\sqrt{k^2+2\sigma}}{2k}[\exp(itk\sqrt{k^2+2\sigma})-\exp(-itk\sqrt{k^2+2\sigma})]\right\}, \tag{10}$$

where $v'\equiv v-v_g$. Equation (9) is the dispersion relation. It indicates that the system is stable or unstable for $\mathrm{sgn}(\mu)<0$ or $\mathrm{sgn}(\mu)>0$ [1].

Equation (10) can be decomposed as the summation of four exponential integrals so that each integral can be carried out by the saddle point method for large t. To realize the decomposition, we need an infinitesimal deformation of the integration path around $k=0$, i.e., along an infinitesimal semicircle above (below) $k=0$. This does not change the value of the integration in Eq. (10) since $k=0$ is an analytic point (removable singularity) of the total integrand, but it does make all four exponential integrals individually well defined. It is evident from Eq. (10) that $k=0$ now becomes a simple pole for two of the four integrands. To evaluate each of the four integrals individually, we need to further deform their integration paths to reach their respective steepest descent paths. On some occasions, the path will come across the simple pole in the deformation process. In such cases, the asymptotic integral value is the contribution from the saddle point and the pole. In the following, however, we will not explicitly decompose Eq. (10) and perform the above procedure. Instead, we only give the final results and concentrate on the physical picture.

We first consider the stable case $\mathrm{sgn}(\mu)>0$. Then the time dependence of the contributions from the saddle points of $kv'\pm k\sqrt{k^2+2}$ in Eq. (10) normally has a decay factor $1/\sqrt{t}$ (or $1/t^{1/3}$ if the group velocity dispersion, i.e., the second order derivative of $kv'\pm k\sqrt{k^2+2}$, is also zero at the saddle point) multiplied by an oscillatory or an exponentially decaying factor [10]. This is expected of an ordinary stable dispersive system, where an initial perturbation tends to disperse and vanish in the space-time domain. However, the simple pole contribution at $k=0$ in the second term in Eq. (10) should also be considered. It actually gives the dominant contribution for large t. This effect is different from the ordinary stable dispersive system. As long as $v'\neq\sqrt{2}$, the saddle points and the pole $k=0$ are separated. It turns out that the pole contribution can be obtained by the lowest-order Taylor expansion of $\pm k\sqrt{k^2+2}$ in the exponential and $\sqrt{k^2+2}$ in the numerator at $k=0$, and we have

$$\delta A(vt,t)\simeq\int\frac{dk}{2\pi}\exp(ikv't)\frac{1}{\sqrt{2}k}\times[\exp(i\sqrt{2}kt)-\exp(-i\sqrt{2}kt)] \tag{11}$$

$$=(i/\sqrt{2})\mathrm{rect}[v'/(2\sqrt{2})] \tag{12}$$

for $t\to\infty$, where the rectangular function $\mathrm{rect}(y)$ is unity if $-\frac{1}{2}<y<\frac{1}{2}$ and zero elsewhere. The decaying saddle point contributions have been neglected in Eqs. (11) and (12). Physically, we notice that the group velocity from the dispersion relation Eq. (9) is always in the ranges $v-v_g<-\sqrt{2}$ and $v-v_g>\sqrt{2}$ for $\mathrm{sgn}(\mu)>0$. Thus the finite level of perturbation within $-\sqrt{2}<v-v_g<\sqrt{2}$ at large t is due to the nonlinear effect.

The above approximation breaks down around $v'=\pm\sqrt{2}$ within a "boundary layer" of v' which shrinks as $t\to\infty$. This is because the saddle point can then be so close to the pole $k=0$ that the magnitude of the saddle point contribution is very large in this parameter region (although still decreasing for large t). Incidentally, zero group-velocity dispersion also corresponds to $v'=\sqrt{2}$. In order to find the solution for this "boundary layer," we need an approximation that is valid even when $v'\simeq\sqrt{2}$. This can be accomplished by keeping the second order terms in the Taylor expansion of $\pm k\sqrt{k^2-2}$ in the exponential since the saddle point contribution for v' around $\sqrt{2}$ is then automatically included. This results in

$$\delta A(vt,t)\simeq\int\frac{dk}{2\pi}\exp(ikv't)\frac{1}{\sqrt{2}k}\{\exp[i\sqrt{2}kt+ik^3t/(2\sqrt{2})]-\exp[-i\sqrt{2}kt-ik^3t/(2\sqrt{2})]\} \tag{13}$$

$$=\frac{i}{\sqrt{2}}\{F[3^{-1/3}\sqrt{2}(\sqrt{2}+v')t^{2/3}]+F[3^{-1/3}\sqrt{2}(\sqrt{2}-v')t^{2/3}]\}\ , \tag{14}$$

for $t\rightarrow\infty$, where the function

$$F(\alpha)=\int(dy/2\pi)[\sin(\alpha y+y^3/3)]/y$$

$$=\tfrac{1}{2}-\int_\alpha^\infty \mathrm{Ai}(y)dy=\int_{-\infty}^{\alpha}\mathrm{Ai}(y)dy-\tfrac{1}{2}\ ,$$

and $\mathrm{Ai}(\alpha)$ is the Airy function defined as

$$\mathrm{Ai}(\alpha)=\int_0^\infty\cos(\alpha y+y^3/3)dy/\pi$$

[10]. Since $F(\alpha)\sim\pm\frac{1}{2}$ for $|\alpha|\gg1$, it can be shown that for a fixed v' not very close to $\pm\sqrt{2}$ this result is identical with the previous derivation. But the result also gives the boundary layer structure. By using $|\alpha|\sim1$, it is easy to see that the thickness of boundary layers about $v'=\pm\sqrt{2}$ decreases as $1/t^{2/3}$ in the normalized spatial coordinate of v. This corresponds to a boundary layer of the order of $t^{1/3}$ in the spatial coordinate x. The structure of the boundary layer is isomorphic with the front of a water wave (or surface-gravity wave) [10].

Figure 1 shows the result for $|\delta A(vt,t)|^2$ from numerical integration of Eq. (10) and our simplified calculations based on Eqs. (14) and (12), which agree well even for the moderately long time $t=15$. Compared with the case of a linear medium [10], this result shows that the development of a localized perturbation will be saturated at a certain level determined by the energy of the initial perturbation, instead of dispersing away. The perturbation will radiate out, as it propagates with v_g, with both shocklike fronts moving out from the center with constant speed $\sqrt{2}$, so the total perturbation energy increases linearly with time. If $v_g<\sqrt{2}$, the perturbation will not vanish after a long time in the laboratory frame as ordinary dispersive waves do.

We now turn our attention to the important case of the

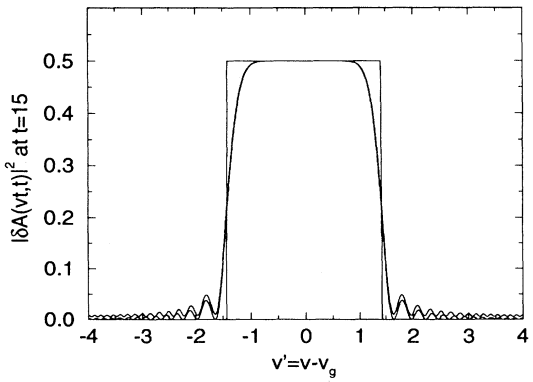

FIG. 1. The shape of the Green function for the modulationally stable system plotted as $|\delta A(vt,t)|^2$ versus $v'\equiv v-v_g$ at $t=15$. The square curve is the approximate result from Eq. (12). The other two curves are the exact result from Eq. (10) (upper curve) and the approximate result from Eq. (14) (lower curve).

modulationally unstable system with $\mathrm{sgn}(\mu)<0$. In such a case, we can prove that the pole $k=0$ in Eq. (10) cannot be a saddle point for any value of v; thus the saddle points and the pole are always separated, and the contribution to the integration at large t is just the summation of the pole contribution and the saddle point contributions. For the unstable portion of v, since the saddle point contributions represent an exponential growth with time, the pole contribution can be neglected. Actually, there are two saddle points from $kv'\pm k\sqrt{k^2-2}$ in Eq. (10) that give contributions growing exponentially with time. Compared to most unstable systems in which only one saddle point contribution has the largest growth rate, here the growth rates of the two contributions are the same while their phases are different. Thus, as will be detailed in the following calculation, the amplitude of the asymptotic pulse is oscillatory with an exponentially growing envelope. This is characteristic of a modulationally unstable system.

For the exponential $kv'+k\sqrt{k^2-2}$ in Eq. (10), the saddle points in the complex k plane satisfy

$$d_k[kv'+k\sqrt{k^2-2}]=0\ . \tag{15}$$

The saddle point with exponentially growing contribution is determined to be

$$k(v)=-[(8+v'^2+v'\sqrt{v'^2-16})/8]^{1/2}\ . \tag{16}$$

Here we concern ourselves with $|v'|<4$ for the unstable portion of the pulse. The value of the exponential $kv'+k\sqrt{k^2-2}$ and its second order derivative at the saddle point can be calculated to be

$$s(v)=k(v)(3v'+\sqrt{v'^2-16})/4 \tag{17}$$

$$=(\sqrt{2}/8)[v'^4+40v'^2-16-v'(v'^2-16)^{3/2}]^{1/2} \tag{18}$$

and

$$p(v)=8k(v)[v'/(v'^2-8-v'\sqrt{v'^2-16})$$

$$-(v'+\sqrt{v'^2-16})/8]\ , \tag{19}$$

respectively. The value of the factor $\sqrt{k^2-2}/k$ in Eq. (10) at the saddle point is

$$d(v)=-\tfrac{1}{4}(v'-\sqrt{v'^2-16})/k(v)\ . \tag{20}$$

In Eqs. (18)–(20), $k(v)$ is given by Eq. (16). Similar results can be obtained for the other exponential $kv'-k\sqrt{k^2-2}$ in Eq. (10).

According to the method of steepest descendant, we add up the two saddle point contributions from $kv'\pm k\sqrt{k^2-2}$. Detailed analysis shows that their contributions are complex conjugates of each other so the final result can be written as

$$\delta A(vt,t)\simeq(1/\sqrt{4\pi t}\,)\mathrm{Re}[e^{is(v)t}/\sqrt{-ip(v)}]+i(1/\sqrt{4\pi t}\,)\mathrm{Im}[e^{is(v)t}d(v)/\sqrt{-ip(v)}] \tag{21}$$

$$=(1/\sqrt{4\pi t}\,)e^{-\mathrm{Im}(s)t}\{\mathrm{Re}[e^{i\,\mathrm{Re}(s)t}/\sqrt{-ip}\,]+i\,\mathrm{Im}[e^{i\,\mathrm{Re}(s)t}d/\sqrt{-ip}\,]\} \tag{22}$$

for $t\to\infty$, where by using Eqs. (18)

$$-\mathrm{Im}(s)=[4(2v'^2+4)^{3/2}+32-40v'^2-v'^4]^{1/2}/8\ , \tag{23}$$

$$\mathrm{Re}(s)=-\mathrm{sgn}(v')[4(2v'^2+4)^{3/2}-32+40v'^2+v'^4]^{1/2}/8\ , \tag{24}$$

as are displayed in Fig. 2. Equation (22) means that the envelope of the asymptotic pulse is determined by $\exp\{-\mathrm{Im}[s(v)]t\}$ [1,9], while the frequency and phase of the amplitude oscillation are determined by $\mathrm{Re}[s(v)]t$, $p(v)$, and $d(v)$. The most important information for the instability is the envelope which gives the asymptotic temporal growth rate $-\mathrm{Im}[s(v)]$ displayed in Fig. 2. Thus the unstable portion of the pulse corresponds to $|v'|<4$. By checking the asymptotic temporal growth rate at $v=0$ [5–8], it is easily found that the instability is convective or absolute for $v_g>4$ or $v_g<4$. This is in agreement with previous results [1,9].

In order to find a simpler expression for the pulse shape, we notice that the predominant portion of the pulse is around $v'=0$ at large t. This allows us to take Taylor expansions for both exponentials and coefficients in Eq. (22) and keep only the lowest-order terms. Then Eq. (22) becomes

$$\delta A(vt,t)\simeq\frac{1+i}{2\sqrt{2\pi t}}\exp[(1-v'^2/8)t]\cos(v't)\ . \tag{25}$$

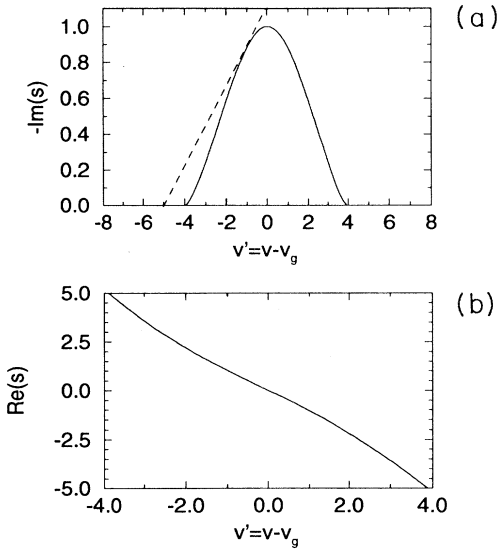

FIG. 2. The real and imaginary parts of the exponential factor $s(v)$ in the saddle point integration. (a) $-\mathrm{Im}[s(v)]$ is the asymptotic growth rate. The slope of the dashed curve corresponds to maximum spatial growth rate for $v_g=5$. (b) $\mathrm{Re}[s(v)]$ is the phase of the oscillations in Fig. 3 below.

The same result can be obtained by a second-order Taylor expansion of the exponentials $\pm itk\sqrt{k^2-2}$ in Eq. (10) around $k=\mp1$, which correspond to their respective maxima. Figure 3 shows the asymptotic pulse shape plotted as $t\exp(-2t)|\delta A(vt,t)|^2$, determined by numerical integration of Eq. (10) and by our simplified Eq. (25). They agree with each other well even for the moderately long time $t=10$.

IV. SPATIAL AMPLIFICATION

Following the systematic approach of the impulse-response analysis [5–8], we now study the spatial growth rate for the convectively unstable case of $\mathrm{sgn}(\mu)<0$ and $v_g>4$. This is accomplished by introducing a point source oscillating at a frequency ω_0 (i.e., zero spectral linewidth), and finding the steady-state spatial solution reached at large t (after a transient time), whose existence is guaranteed by the convective nature of the instability. The amplification of a signal with arbitrary linewidth can be studied in terms of spectrum decomposition. Thus we assume $S(t)=\exp(-i\omega_0)t$ in Eq. (4) or $\bar{S}(\omega)=[i(\omega-\omega_0)]^{-1}$ in Eq. (7). In this analysis, we use the spatial coordinate x instead of the normalized spatial coordinate of v since we are concerned with the steady state.

Following the standard approach [5–8], we move the integration path of ω below its real axis. Due to the absence of absolute instability, the k integration path can always be deformed so that the solution at large t is only due to the pole of ω at ω_0 and can be expressed as

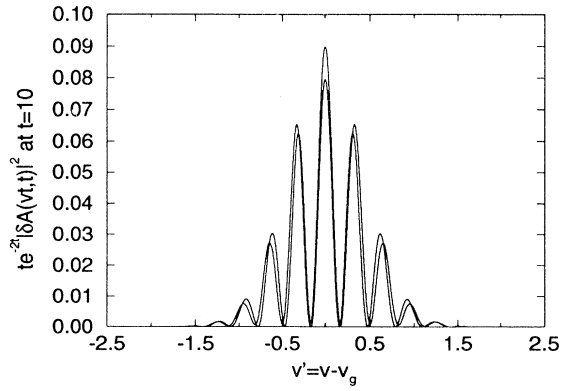

FIG. 3. The shape of the Green function for the modulationally unstable system plotted as $t\exp(-2t)|\delta A(vt,t)|^2$ versus $v'\equiv v-v_g$ at $t=10$. The two curves are the exact result from Eq. (10) (upper curve) and the approximate result from Eq. (25) (lower curve).

$$\delta A(x,t)\simeq\int_L \frac{dk}{2\pi}\exp(ikx)\frac{-(\omega_0-v_gk+k^2-1)\exp(-i\omega_0t)+\exp(i\omega_o t)}{k^2(k^2-2)-(\omega_0-v_bk)^2} \quad \text{for } t\to\infty \tag{26}$$

where L is the Landau contour. (For a detailed discussion, see [6].) This steady-state solution can be reached for any fixed spatial coordinate x after a transient time. Physically, the new frequency component of $\exp(i\omega_0 t)$ is generated by the four-wave mixing process.

The integration in Eq. (26) can be worked out for $x>0$ and $x<0$ separately. For simplicity we only consider $x>0$ since the case $x<0$ is similar. Then the integration with k in Eq. (26) is just the residue summation from all the poles of the integrand above the Landau contour. For large x, only the lowest pole at k_0 gives a dominant contribution, that is,

$$\delta A(x,t)\simeq\exp[ik_0x]\frac{-(\omega_0-v_gk_0+k_0^2-1)\exp(-i\omega_0t)+\exp(i\omega_0t)}{4k_0(k_0^2-1)+2v_g(\omega_0-v_gk_0)} \quad \text{for } t\to\infty \tag{27}$$

where $k_0(\omega_0)$ is a function of ω_0 and satisfies

$$k_0^2(k_0^2-2)-(\omega_0-v_gk_0)^2=0\ . \tag{28}$$

For amplification, $k_0(\omega_0)$ should be below the real axis while still above the Landau contour. This criterion is equivalent to the requirement that the corresponding solutions of Eq. (28) cross the real axis from above to below when we attach an imaginary part to ω_0 that goes from some positive value to zero (for detailed discussion, see [6]).

The solutions of Eq. (28) are of course functions of ω_0. A detailed study shows that for $v_g>4$ there are two separate regions for positive ω_0, namely $(0,\omega_a)$ and (ω_e,∞), that result in complex solutions of Eq. (28). However, only the first region corresponds to amplification. By applying the above criterion, it can be shown that the second one corresponds to evanescent waves. The same is true for negative ω_0 due to symmetry. As an example, Fig. 4 shows all four solution branches of Eq. (28) for varying ω_0 and $v_g=5$, where we have used the normalized frequency $\Omega_0=\omega_0/v_g$, and chosen the attached imaginary part to Ω_0 to be 0.4, 0.1, and 0, while its real part can be at some discrete values which are 0.1 apart in the range $(-5,5)$. Thus only the portion of the bow-shaped curve below the real axis in Fig. 4(d) has come across the real axis and corresponds to amplification. This portion of k_0 corresponds to the Ω_0 range of $(-1.35,1.35)$, i.e., $\Omega_a=\omega_a/v_g=1.35$.

By solving Eq. (28), Fig. 5 shows the wave number $\mathrm{Re}[k_0(\omega_0)]$ as $\mathrm{Re}[k_0(\omega_0)]-\Omega_0$ and the spatial growth rate $-\mathrm{Im}[k_0(\omega_0)]$ as $-v_g\mathrm{Im}[k_0(\omega_0)]$ for $v_g<4$ in the amplification range of Ω_0. Figure 6 shows the amplification range Ω_a, the maximum growth rate as $v_g\max[-\mathrm{Im}(k_0)]$, and corresponding frequency $\Omega_m=\omega_m/v_g$ for different v_g. While the wave number $\mathrm{Re}(k_0)$ approaches Ω_0, the quantities $v_g\max[-\mathrm{Im}(k_0)]$ and Ω_m decrease to approach 1, and the normalized amplification frequency range Ω_a increases to approach $\sqrt{2}$, as v_g increases. It should be pointed out that $\max[-\mathrm{Im}(k_0)]$ for a given v_g is equal to the slope of the tangential line shown in Fig. 2(a) (where we have used $v_g=5$ as an example) as can be generally proved [5–8].

The branch of the solution of Eq. (28) related to amplification can be obtained directly by treating v_g^{-2} as a small parameter since we have assumed $v_g>4$. By writing Eq. (28) in the form

$$(k_0-\Omega_0)^2=v_g^{-2}(k_0^4-2k_0^2)\ , \tag{29}$$

it is easy to see that the zeroth-order solution is $k_0=\Omega_0$. The next order solution will be accurate to $O(v_g^{-1})$ and can be obtained by the zeroth-order Taylor expansion of

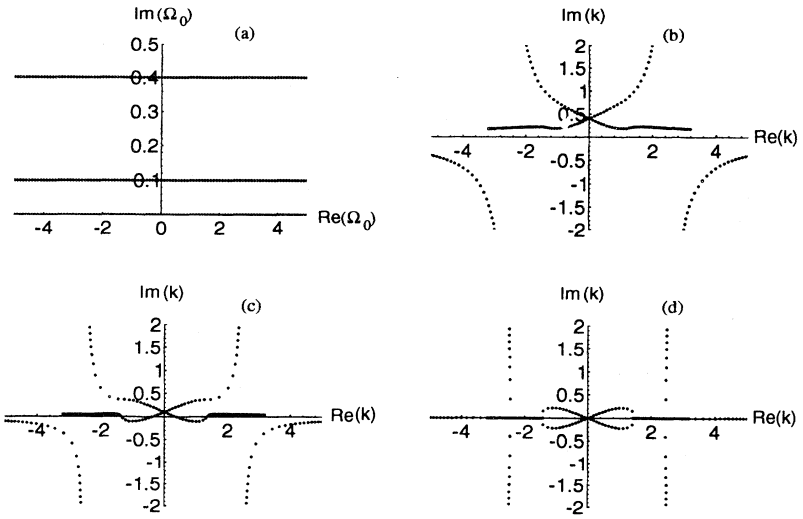

FIG. 4. The four branches of the dispersion relation satisfying Eq. (28) for $v_g=5$ and a varying parameter ω_0. (a) The values of the parameter $\Omega_0=\omega_0/v_g$ are dotted on the three horizontal lines at $\mathrm{Im}(\Omega_0)=0.4$ (first), 0.1 (second), and 0 (third) with separation of 0.1 between the dots. (b) The four branches of the solution of Eq. (28) for the values of Ω_0 on the first line in (a). (c) Same as (b) except for the second line in (a). Note the part that crosses the real axis. (d) Same as (b) except for the third line in (a). Thus k_0 is on the bow-shaped curve below the real axis.

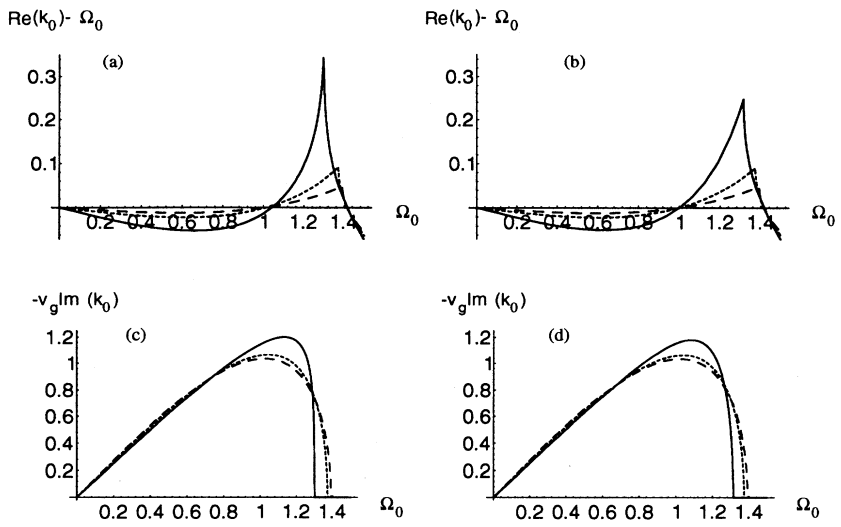

FIG. 5. The spatial growth rate and corresponding wave number for varying frequency in the amplification range and for $v_g=4$ (solid), 6 (dashed), and 8 (long dashed). The wave number is plotted as $\mathrm{Re}(k_0)-\Omega_0$ versus $\Omega_0=\omega_0/v_g$ in (a) and (b), and the spatial growth rate is plotted as $-v_g\mathrm{Im}(k_0)$ versus Ω_0 in (c) and (d), where (a) and (c) are the exact results from Eq. (28) and (b) and (d) are the approximate results from Eq. (31).

the right-hand side of Eq. (29) at $k_0=\Omega_0$. After taking the square root on both sides of the resulting equation, we have

$$k_0(\omega_0)\simeq\Omega_0-v_g^{-1}\Omega_0\sqrt{\Omega_0^2-2}\ . \tag{30}$$

Thus $\Omega_a=\sqrt{2}$, $\Omega_m=1$, and $v_g\max[-\mathrm{Im}(k_0)]=1$ in agreement with the results in Figs. 5 and 6 for $v_g\gg1$. This result can also be obtained from another version of the NSE used to study the boundary input problem, i.e.,

$$\partial_{x'}a=-v_g'^{-1}\partial_{t'}a-i(\beta_2/2)\partial_{t't'}^2a+i\gamma|a|^2a\ ,$$

where $\beta_2=2\mu/(v_g')^3$ and $\gamma=\lambda/v_g'$. The two versions are equivalent only when $v_g=v_g'/\sqrt{a_0^2\lambda|\mu|}\gg1$.

The accuracy can be improved by considering the second-order Taylor expansion of the right-hand side of Eq. (29) at $k_0=\Omega_0$. In fact, one can prove that the solution thus obtained is at least accurate to $O(v_g^{-3})$ with higher accuracy around $\Omega_0=0$ and $\Omega_0=\sqrt{2}$. The resulting second order algebraic equation for k_0 can be easily solved to give

$$k_0(\omega_0)-\Omega_0\simeq\frac{2v_g^{-2}\Omega_0(\Omega_0^2-1)-v_g^{-1}\Omega_0\sqrt{\Omega_0^2-2+2v_g^{-2}(-\Omega_0^4+3\Omega_0^2)}}{[1-2v_g^{-2}(3\Omega_0^2-1)]}\ . \tag{31}$$

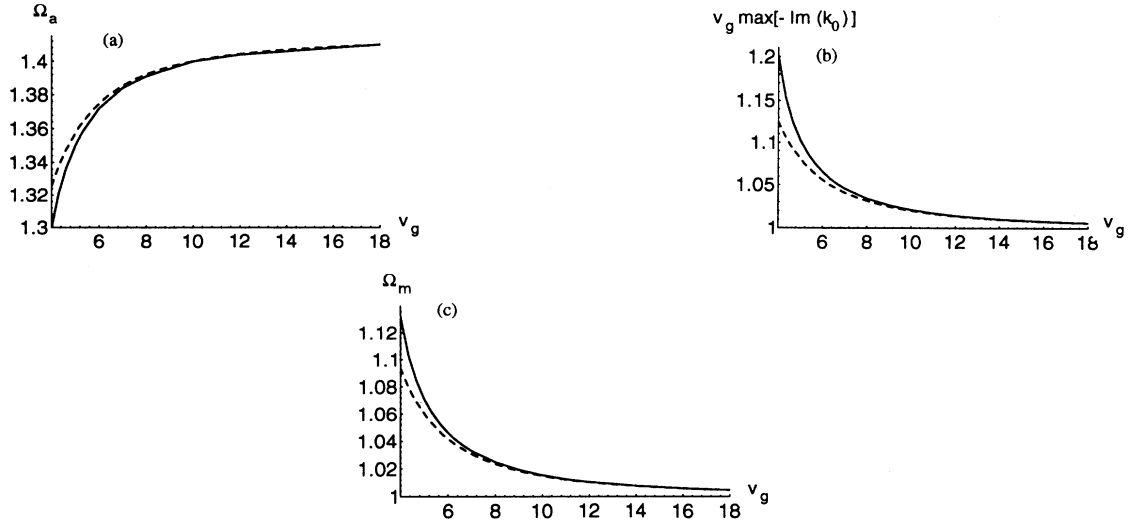

FIG. 6. The amplification frequency range plotted as $\Omega_a=\omega_a/v_g$ (a), the maximum spatial growth rate plotted as $v_g\max[-\mathrm{Im}(k_0)]$ (b), and the corresponding frequency plotted as $\Omega_m=\omega_m/v_g$ (c) for varying v_g (c). The solid lines are from numerical calculations based on Eq. (28) and the dashed lines are from the approximate analytical calculations based on Eqs. (32), (34), and (35).

Equation (31) is quite accurate, as shown in Fig. 5.

The frequency range for the amplification can be easily obtained from Eq. (31) by setting the term under the square root to zero, and the solution is

$$\Omega_a \simeq \sqrt{2}(1-v_g^{-2}) \tag{32}$$

where we have Taylor expanded the result up to the $O(v_g^{-2})$ term.

According to Eq. (31), the maximum growth rate $\max[-\mathrm{Im}(k_0)]$ and the corresponding frequency Ω_m can be obtained by studying the extremum of

$$\frac{-v_g^{-1}\Omega_0\sqrt{\Omega_0^2-2+2v_g^{-2}(-\Omega_0^4+3\Omega_0^2)}}{[1-2v_g^{-2}(3\Omega_0^2-1)]} \simeq -v_g^{-1}\sqrt{y^2-1+2v_g^{-2}(5y^3+4y^2-3y-2)}\ , \tag{33}$$

where $y=\Omega_0^2-1$ and Taylor expansion has been made up to $O(v_g^{-2})$. The extremum of the argument under the square root of the right-hand side of Eq. (33) can be easily found by using ordinary perturbation with respect to v_g^{-2}. After some straightforward algebra, we obtain

$$\Omega_m \simeq 1+\tfrac{3}{2}v_g^{-2}\ , \tag{34}$$

$$v_g \max[-\mathrm{Im}(k_0)] \simeq 1+2v_g^{-2}\ , \tag{35}$$

where we have kept the expansions up to the $O(v_g^{-2})$ term.

Equations (32), (34), and (35) are good approximations as long as $v_g^2 \gg 1$. The comparison with the numerical solution is displayed in Fig. 6.

V. CONCLUSION

We reported the result of impulse-response analysis for a nonlinear wave in a dispersion medium. The Green function for a pulselike perturbation and the solution for oscillatory perturbations were studied. For a modulationally unstable system, the asymptotic pulse not only grows but is also modulated, i.e., the perturbation pulse consists of a modulation structure whose envelope grows exponentially. The pulse shape and the condition for convective and absolute instability were obtained analytically. Even for a modulationaly stable nonlinear dispersive system, the perturbation does not disperse away as it does in a linear system. Instead, a certain level of perturbation determined by the energy of the initial pulse occurs in a widening region of space whose center moves with the group velocity. In a sense, it is like a spreading square pulse. For an oscillatory perturbation source, we determined the frequency regions for amplification and evanescence. The spatial growth rates for amplifying waves were obtained. The results also showed that the spatial NSE and temporal NSE are equivalent only for $v_g \gg 1$.

ACKNOWLEDGMENTS

The research of C. J. McKinstrie and M. Yu was supported by the National Science Foundation under Contract No. PHY-9057093, the U.S. Department of Energy (DOE) Office of Inertial Confinement Fusion under Cooperative Agreement No. DE-FC03-92SF19460, the University of Rochester, and the New York State Energy Research and Development Authority.

[1] C. J. McKinstrie and G. G. Luther, Phys. Scr. **T30**, 31 (1990), and references therein.

[2] A. Hasegawa, *Plasma Instabilities and Nonlinear Effects* (Springer-Verlag, Berlin, 1975).

[3] G. P. Agrawal, *Nonlinear Fiber Optics,* 2nd ed. (Academic, San Diego, 1995).

[4] A. D. D. Craik, *Wave Interactions and Fluid Flows* (Cambridge University Press, Cambridge, UK, 1985).

[5] R. J. Briggs, *Electron-Stream Interaction with Plasmas* (MIT Press, Cambridge, MA, 1964), Chap. 2.

[6] E. M. Lifshitz and L. P. Pitaevskii, *Physical Kinetics* (Oxford University Press, New York, 1981), p. 265.

[7] A. Bers, in *Basic Plasma Physics,* edited by A. A. Galeev and R. N. Sudan, Handbook of Plasma Physics, Vol. 1 (North-Holland, Amsterdam, 1983), p. 451.

[8] P. Huerre, in *Instabilities and Nonequilibrium Structures,* edited by E. Tirapegui and D. Villarroel (Reidel, New York, 1987), p. 141.

[9] M. Yu and C. J. McKinstrie, Bull. Am. Phys. Soc. **37**, 1441 (1992).

[10] G. B. Whitham, *Linear and Nonlinear Waves* (Wiley, New York, 1974), p. 442.